Cellular and Molecular Life Sciences (2020) 77:2217–2233
https://doi.org/10.1007/s00018-019-03282-3

ORIGINAL ARTICLE

Tetraspanin1 promotes NGF signaling by controlling TrkA receptor proteostasis

Facundo Ferrero Restelli[1] · Paula Aldana Fontanet[1] · Ana Paula De Vincenti[1] · Tomás Luis Falzone[2] · Fernanda Ledda[1,3] · Gustavo Paratcha[1]

Received: 1 February 2019 / Revised: 6 August 2019 / Accepted: 15 August 2019 / Published online: 22 August 2019

Abstract

The molecular mechanisms that control the biosynthetic trafficking, surface delivery, and degradation of TrkA receptor are essential for proper nerve growth factor (NGF) function, and remain poorly understood. Here, we identify Tetraspanin1 (Tspan1) as a critical regulator of TrkA signaling and neuronal differentiation induced by NGF. Tspan1 is expressed by developing TrkA-positive dorsal root ganglion (DRG) neurons and its downregulation in sensory neurons inhibits NGF-mediated axonal growth. In addition, our data demonstrate that Tspan1 forms a molecular complex with the immature form of TrkA localized in the endoplasmic reticulum (ER). Finally, knockdown of *Tspan1* reduces the surface levels of TrkA by promoting its preferential sorting towards the autophagy/lysosomal degradation pathway. Together, these data establish a novel homeostatic role of Tspan1, coordinating the biosynthetic trafficking and degradation of TrkA, regardless the presence of NGF.

Keywords Neurotrophins · TrkA · Tetraspanins (Tspans) · Sensory neurons · Neuronal differentiation and receptor proteostasis

Abbreviations

CNX	Calnexin
DRG	Dorsal root ganglia
ER	Endoplasmic reticulum
Erk	Extracellular signal-regulated kinase
GDNF	Glial cell line-derived neurotrophic factor
Lamp1	Lisosomal-associated membrane protein 1
NGF	Nerve growth factor
PNS	Peripheral nervous system
P75NTR	p75 neurotrophin receptor
Ret	Rearranged in transformation
RTK	Receptor tyrosine kinase
TBP	TATA-binding protein
TEMs	Tetraspanin-enriched microdomains
TrkA	Tropomyosin-related kinase A
Tspan	Tetraspanin

Electronic supplementary material The online version of this article (https://doi.org/10.1007/s00018-019-03282-3) contains supplementary material, which is available to authorized users.

✉ Gustavo Paratcha
gparatcha@fmed.uba.ar

[1] División de Neurobiología Molecular y Celular, Instituto de Biología Celular y Neurociencias (IBCN)-CONICET-UBA, Facultad de Medicina, University of Buenos Aires (UBA), CP1121 Buenos Aires, Argentina

[2] Laboratorio de Transporte Axonal y Enfermedades Neurodegenerativas, Instituto de Biología Celular y Neurociencias (IBCN)-CONICET-UBA, Facultad de Medicina, University of Buenos Aires (UBA), CP1121 Buenos Aires, Argentina

[3] Fundación Instituto Leloir, Instituto de Investigaciones Bioquímicas de Buenos Aires (IIBBA), CONICET, Buenos Aires, Argentina

Introduction

In the peripheral nervous system (PNS), the generation of neural circuitry underlying somatosensory perception relies on intricate coordination of axonal growth, branching, guidance, target recognition, synapse formation, and survival of morphologically and functionally distinct subtypes of sensory neurons [1–3]. Target-derived neurotrophic factors, such as nerve growth factor (NGF) and glial cell line-derived neurotrophic factor (GDNF), have been shown to contribute to the establishment of neuronal connectivity, signaling through TrkA and Ret receptor tyrosine kinases, respectively [4, 5]. Trk and Ret receptors are expressed in specific subpopulations of sensory, sympathetic, and spinal cord motor neurons where they control

axonal extension, target innervation, and survival [6–9]. Although these receptors are expressed in specific subsets of neurons, they are not able by themselves to determine the specificity of axonal connectivity and peripheral tissue innervation. Cooperative mechanisms between neurotrophic factors and other axon guidance/branching extracellular cues (such as Wnts, Semaphorins, and Slits) have provided insights into how a relatively small number of neurotrophic factors can generate target specificity during neuronal circuit formation [1, 10, 11]. Various genetically modified mouse models have demonstrated that Trk and Ret receptor signals need to be modulated to confer cell-type specific responses to their respective ligands during circuit development. Receptor-associated proteins, such as Lrig1 (leucine-rich repeat and Immunoglobulin-like domain protein 1), Linx (leucine-rich repeat domain and immunoglobulin domain containing axon extension protein), and PTPRO (protein tyrosine phosphatase receptor type O), enhance or restrict neurotrophic activity to regulate axonal growth and target innervation during PNS development [2, 12–14]. It is likely that other cell-type specific receptor components or modulators of neurotrophic actions can contribute to axonal growth and target innervation in the peripheral nervous system.

Tetraspanins (Tspans) constitute a superfamily of under-characterized cell-surface proteins with four transmembrane domains, two extracellular loops, and two short cytoplasmic tails. They have the ability to associate with different receptors, signaling molecules and among themselves, forming a distinct class of membrane domains, named tetraspanin-enriched microdomains (TEMs). Tspans regulate a variety of cellular processes including intracellular trafficking, cell adhesion, migration, and differentiation. By virtue of their capacity to laterally interact with membrane receptors, Tspans also function as inhibitors or facilitators of growth factor receptor signaling [15–21].

Tetraspanins have been extensively studied in several biological processes spanning from the immune system to tumor growth regulation [22]. Although the functional contribution of tetraspanins during nervous system development is still at an early stage, in the last few years, several studies on this subject have established that tetraspanins are key regulators of a large group of proteins involved in synapse formation, function, and plasticity [23–28]. These observations prompted us to investigate whether Tspans might represent novel modulators of neurotrophic factor receptor signaling.

Here, we performed a plasmid-based screening method to identify Tspan-family members critically involved in NGF/TrkA-mediated neurite outgrowth. In addition, we present mechanistic evidence demonstrating that Tspan1 facilitates NGF-dependent signaling responses by controlling the biosynthetic trafficking and proteostasis of TrkA.

Materials and methods

Cell lines, recombinant proteins, and inhibitors

PC12 cells were grown in DMEM supplemented with 5% horse serum and 10% FBS (Invitrogen). COS and HEK-293 cells were grown in DMEM supplemented with 10% FBS as previously described [29]. NGF and bFGF were purchased from Promega and R&D systems, respectively. The pan-caspase inhibitor Z-VAD-FMK was purchased from Sigma. The autophagy-lysosomal inhibitors Chloroquine and NH_4Cl were from Sigma and Bafilomycin A1 was obtained from Tocris.

Real-time PCR

The developmental expression of *Tspan1* and *TATA box binding protein (Tbp)* mRNAs was analyzed by real-time PCR. Total RNA was isolated from DRG ganglia obtained at different developmental stages using RNA-easy columns (Quiagen). cDNA was synthesized using Multiscribe reverse transcriptase and random hexamers (Applied Biosystems). The cDNA was amplified using the following primer sets: TATA box binding protein (*Tbp*): forward, 5´-GGG GAG CTG TGA TGT GAA GT-3; reverse, 5´-CCA GGA AAT AAT TCT GGC T´CA-3´ [30]; Rat *Tspan1*: forward, 5´-TGG CTG AAC AAT TCC TGA CA-3;´ reverse, 5´-CCC TCC ATC GTA GAG TTC CA-3;´ The specificity of the primers was controlled by conventional PCR. Real-time PCR was performed using the SYBR Green qPCR Master Mix (Invitrogen) on an ABI7500 sequence detection system (Applied Biosystems), according to the manufacturer's instructions. Reactions were performed in 25 µl volume. Nucleotides, Taq DNA polymerase, and buffer were included in the SYBR Green Master Mix (Invitrogen).

Cell transfection, plasmids, and pharmacological treatments

COS and HEK-293 cells were transfected with Polyethylenmine-PEI (Polysciences). PC12 cells were transfected using X-tremeGENE (Roche) following the manufacturer's instructions. PC12-Flag-Tspan1 clon (T7) was generated by isolation of colonies transfected with the full-length Myc-tagged-Tspan1 construct and selected with neomycin.

Transient transfection of primary dorsal root ganglion (DRG) neurons was performed using Lipofectamine 2000 (Invitrogen) in 300 µl of DMEM:F12 serum-free medium containing 1 µg of total plasmid DNA per well in 24-well plates containing 1.5×10^5 cells/well. For downregulation experiments, DRG sensory neurons were transfected with 1

μg of *Tspan1*-shRNA constructs expressing GFP protein. For overexpression experiments, PC12 cells were co-transfected with different epitope-tagged Tspan (0.9 μg) constructs and GFP expression vector (0.1 μg) per well in 24 well plates containing 0.6–0.75 × 10^5 cells/well.

Tspan1-shRNA-GFP and Flag-tagged-rat Tspan1 were purchased from Cellogenetics, Inc. The vector pRetro-U6G shRNA was transfected for expression of *Tspan1*-shRNA targeting rat *Tspan1*. Flag-tagged-rat Tspan1 was cloned in pRPCX1.0 vector. Plasmid cDNA encoding full-length Myc-DDK-tagged rat Tspan1, Myc-DDK-tagged human Tspan1, Myc-DDK-human Tspan3, Myc-DDK-mouse Tspan5, and Myc-DDK-mouse Tspan7 were purchased from Origene Technologies. Plasmids encoding Flag-Tspan9, Flag-CD9, and Flag-CD63 were kindly provided by Dr. Michael G. Tomlinson (University of Birmingham, UK). Plasmid for HA-tagged TrkA-L213P was generously provided from Dr. M. Vilar (Institute of Biomedicine of València, Spain). Lamp1-RFP was kindly provided by Dr. David Sabatini (Whitehead Institute for Biomedical Research, USA). Plasmid encoding GFP was obtained from Clontech.

For downregulation of Tspan1, PC12 cells were transfected with *Tspan1*-shRNA-GFP vector and selected with puromycin to enrich in a pool of transfected cells. PC12 cells were treated independently with Chloroquine (50 μM, Sigma) for 16 h, with NH_4Cl (50 mM, Sigma) for 6 h and with Bafilomycin A1 (400 nM, Tocris) for 6 h. The cell-permeant pan-caspase inhibitor Z-VAD-FMK (Sigma) [29] was used at 50 nM.

Sensory neuron cultures

Dorsal root ganglion (DRG) neurons from embryonic day 15 (E15) Wistar rats of either sex (School of Pharmacy and Biochemistry, University of Buenos Aires) were prepared as previously described [29]. Briefly, the ganglia were dissociated with collagenase (2% wt/v, Sigma), trypsin (0.1% wt/v, Invitrogen), and DNAseI (10 μg/ml, Invitrogen), and then seeded onto poly-ornithine (Sigma) and laminin (Sigma) coated plates. The neurons were maintained in DMEM:F12 medium supplemented with 60 mg/ml penicillin, 100 mg/ml streptomycin, 2 mM glutamine (Invitrogen), 1 mg/ml BSA (Sigma), and NGF (50 ng/ml).

Immunopreciptation and Western blotting

Cells were lysated at 4 °C in buffer containing 0.5% Triton X-100, 1% octylglucoside plus complete EDTA-free protease inhibitor cocktail used according to the manufacturer's instructions (Roche) and phosphatase inhibitors (sodium orthovanadate 1 mM and sodium fluoride 20 mM). Protein lysates were clarified by centrifugation and analyzed by immunoprecipitation and Western blotting as previously described [12]. The blots were scanned in a Storm 845 PhosphorImager (GE Healthcare Life Sciences), and quantifications were done with ImageQuant software (Molecular Dynamics). Numbers below the lanes indicate fold of induction relative to control normalized to total levels of target protein.

The primary antibodies were obtained from various sources as follows: anti-Tetraspanin1 (1/500) was from Proteintech, anti-Myc (1/800) (9E10), anti-actin (1/800) was from Santa Cruz Biotechnology, anti-TrkA (1/1000) was from R&D Systems, anti-Flag M2 antibody (1/1000) was from Sigma, anti-HA antibody (1/1000) was from Roche, anti-phospho TrkA (Tyr490) (1/2000) and anti-phospho MAPK (Erk1/2) (Thr202/Tyr204) (1/2500) were from New England Biolabs, anti-biotin (1/2000) was from Jackson ImmunoResearch, and anti-βIII-tubulin (1/5000) was from Promega.

Cell-surface biotinylation assay

Parental and *shTspan1*-PC12 cells were washed sequentially with room-temperature PBS and cold PBS, chilled on ice, and incubated in 0.5 g/ml of Sulfo-NHS-SS-biotin (Pierce) dissolved in biotinylation buffer (PBS, 1 mM $CaCl_2$, and 0.5 mM $MgCl_2$) for 30 min at 4 °C to label the membrane proteins. Free biotin was quenched with 0.1 M glycine and then washed three times with cold PBS and lysed as indicated above. Cell extracts were immunoprecipitated with anti-pan Trk (C15, Santa Cruz) antibodies. Biotinylated TrkA was detected by TrkA immunoprecipitation and probing with anti-biotin antibody (dil 1/1000).

Trypsin digestion and Triton X-100 solubility assays

Assays were performed as previously described [31]. Briefly, trypsin digestion assay was done by incubating soluble lysates with four increasing concentrations of trypsin (0.5, 1.0, 1.5, and 2.0 μg/μl) on ice for 10 min. The reaction was stopped by adding 2X SDS-PAGE sample buffer and boiled for 5 min.

Immunofluorescence

Cryostat sections of rat embryos at different developmental stages, dissociated DRG neurons, or transfected PC12 cells were fixed with 4% PFA, permeabilized with 0.25% Triton X-100 blocked with 10% donkey serum (Jackson ImmunoResearch) and then incubated with different primary antibodies. The antibodies used in this work included: polyclonal anti-TrkA (dilution 1/200 on tissue sections and 1/1000 cultured cells, R&D systems), anti-Tspan1 (16058-1-AP) (dilution 1/25 on tissue sections and 1/200 on cultured cells, Proteintech), anti-hTspan1 (clone TSP13/

SAB4200484) (dil 1/1500 on cultured cells, Sigma), anti-Calnexin (dilution 1/1500, Sigma), anti-GFP (dilution 1/1000, Invitrogen), and anti-phospho TrkA (dilution 1/2500 on PC12 cells, Cell Signaling). Secondary antibodies were from Jackson ImmunoResearch (dilution 1/300). For each developmental stage, lumbar DRGs coming from 4–6 rats were isolated and embedded in OCT tissue embedding medium. 20 µm serial cryosections were made through the entire DRG and counted every 30 µm. Photographs were obtained using an Olympus IX-81 inverted or an Olympus Confocal microscope.

Image acquisition and quantification

Confocal images from Dorsal Root Ganglia were obtained using a Confocal Olympus FV1000 20x/0.75 objective with sequential acquisition setting. Confocal images for co-localization quantification were obtained using an Olympus IX83 DSU 60x/1.42 NA immersion oil objective with sequential acquisition setting. Images were acquired using the same settings with no saturation and no bleedthrough and minimized noise at a resolution of 1599 × 1186 pixels (16 bit). Images were analyzed using the ImageJ plugin Coloc2. Pearson Correlation Coefficient measured for individual cells using a hand-drawn ROI followed by a Costes' Significance Test was chosen as the co-localization readout. Images for extracellular quantification of TrkA were obtained using an Olympus IX-81 40x/1.42 NA objective. Images were acquired using the same settings with no saturation and no bleedthrough and minimized noise at a resolution of 1360 × 1024 pixels. Images were analyzed using the Fiji ImageJ software and Corrected Total Cell Fluorescence (CTCF) was calculated for each individual cell using a hand-drawn ROI. CTCF is calculated as the integrated density of the selected cell minus the area of the selected cell times the mean fluorescence of background readings [CTCF = IntDen − (Area × MeanBck)].

Neurite outgrowth assays

For PC12 cell differentiation assays, the cells were transfected with different plasmid cDNAs encoding full-length epitope-tagged Tetraspanins and *Tspan1*-shRNAs using X-tremeGENE reagent in complete medium. The next day, the cells were plated on 24-multiwell plates and cultured in DMEM medium (control condition) or DMEM supplemented with NGF (50 ng/ml). After 24, 48, or 72 h, the cells were fixed with 4% paraformaldehyde (PFA). The number of cells bearing neurites longer than 1 or 2 cell bodies (as specified) was quantified relative to the total number of cells counted in at least ten random fields of three different wells in each experiment. PC12 cell differentiation was evaluated in three independent experiments. The pictures were obtained using an Olympus IX-81 inverted microscope.

Neurite outgrowth assays were performed in dissociated cultures of E15 rat DRG neurons. Primary cultures were prepared as previously described (see above). Neurons were transfected with control-shRNA-GFP or *Tspan1*-shRNA-GFP vectors and cultured in the presence of NGF (50 ng/ml) for 36 h. Then, cells were fixed with 4% PFA and stained with anti-GFP and anti-βIII-tubulin to identify neuronal cells. Neuronal survival was evaluated using the nuclear stain 4′,6-diamino-2-phenylindole (DAPI) (Sigma). GFP-positive neurons containing fragmented or condensed nuclear staining were scored as apoptotic cells and not computed in the differentiation assays. Quantification of neurite length was performed using NIH ImageJ software. The pictures were obtained using an Olympus IX-81 inverted microscope.

shRNA-mediated knockdown assays

Rat *Tspan1*-shRNA-GFP expression vectors were purchased from Cellogenetics, Inc. The retroviral vector pRetro-U6G shRNA was used for expression of *Tspan1*-shRNA targeting rat *Tspan1*. The target sequence of the *Tspan1*-shRNA 1 (indicated as sh1) is 5′-GCT GGT GCT GTA CTC TTT ATT-3´, and corresponds to nucleotides 315–335 of rat Tspan1 mRNA. The target sequence of the *Tspan1*-shRNA 2 (sh2) is 5´-GCT GTG GCT TCA ACA ATT ACA-3´, and corresponds to nucleotide 574-594 of rat *Tspan1* mRNA. These regions were not homologous to other Tspans or other known genes determined by a BLAST search. The efficiency of Tspan1 knockdown was confirmed by western blot of cell extracts obtained from transfected COS cells.

Statistical analysis

Data are reported as mean ± SEM or SD as indicated, and significance was accepted at $p < 0.05$. Student's t test or ANOVA was performed using GraphPad Prism 5.0 software.

Results

Tspan1 regulates neuronal differentiation in response to NGF

To characterize the role of Tspans in NGF-induced neuronal differentiation, we used the rat pheochromocytoma cell line PC12, which express both $p75^{NTR}$ and TrkA receptors and differentiate into a neuronal type resembling sympathetic neurons in response to NGF. Thus, the neuroblast-like PC12 cells provide a robust cellular model for studies of NGF activity. To explore a potential role of Tspans

in NGF-induced neuronal differentiation, we performed a plasmid-based method to acutely overexpress several Tspan-family members, such as Tspan1, Tspan3, Tspan5, Tspan7, Tspan9, CD9, and CD63. In particular, these Tspans are expressed in the nervous system and some of them have been implicated in the modulation of tyrosine kinase receptor signaling [16, 25, 32–35]. PC12 cells were transfected with control or epitope-tagged Tspans in combination with an enhanced GFP expression vector. Cells were maintained in the presence of NGF for 24 or 72 h and analyzed for neurite outgrowth response. In these experiments, we found that expression of exogenous Tspan1, but not other Tspans, was sufficient to promote neurite outgrowth after 24 h, and that this effect was also evident after 72 h of treatment with NGF (Fig. 1a–c). Thus, our findings indicate that Tspan1 specifically promote morphological differentiation of PC12 cells in response to NGF.

Next, we performed loss-of-function assays to additionally confirm the role of Tspan1 in NGF-induced neurite outgrowth. To perform these experiments, PC12 cells were transiently transfected with vectors containing two specific shRNAs directed to the rat *Tspan1* mRNA sequence, and

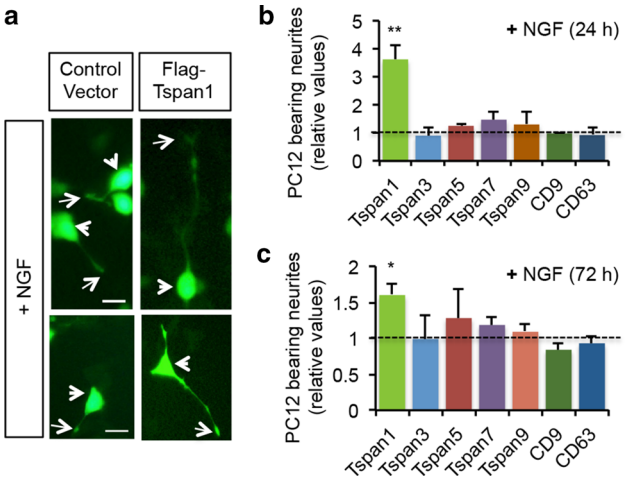

Fig. 1 Overexpression of Tspan1 potentiates PC12 cell differentiation in response to NGF. **a** Photomicrographs show PC12 cell transfected with control or Flag-tagged Tspan1 constructs together with a GFP expression vector. After 24 h maintained in the presence of NGF (50 ng/ml), cells were fixed and analyzed. Arrowheads indicate neuronal cell bodies (CBs) and arrows denote neurite tips. Scale bar, 15 µm. **b** Quantification of the relative number of GFP-positive neurite-bearing PC12 cells longer than 2 CB diameters in the different experimental groups after 24 h of NGF treatment. The results are shown as means ± SD of three independent experiments. Dashed line indicates differentiation value of control vector transfected cells treated with NGF. $^{**}p \leq 0.005$ by Student's *t* test. **c** Quantification of the relative number of GFP-positive neurite-bearing PC12 cells longer than 2 CB diameters in the different experimental groups after 72 h of NGF treatment. The results are shown as means ± SD of three independent experiments. Dashed line indicates differentiation value of control transfected cells treated with NGF. $^{*}p \leq 0.05$ by Student's *t* test

then stimulated with NGF or bFGF during 48 h. Since bFGF also promotes the formation of neurites in PC12 cells, we examined whether downregulation of Tspan1 could also affect outgrowth in response to bFGF. In line with results shown in Fig. 1, knockdown of *Tspan1* by RNA interference abrogated NGF-induced, but not bFGF-promoted neurite outgrowth in PC12 cells, indicating that the effect of Tspan1 was specific on the morphological differentiation induced by NGF (Fig. 2a, b). The efficiency of rat Tspan1 downregulation was confirmed by immunoblotting. These two *shRNAs* were able to abolish the levels of ectopically expressed Tspan1 protein in COS cells (Fig. 2c).

To minimize off-target effects of shRNA, we performed experiments to verify the specificity of the *Tspan1-shRNA* phenotype by testing the ability of an shRNA-resistant human Tspan1 (hTspan1) to rescue the reduced NGF-promoted neurite outgrowth observed upon knockdown of rat Tspan1. We found that hTspan1 was sufficient to reverse this phenotype, suggesting that this effect is due to the specific downregulation of endogenous Tspan1 (Fig. 2d). The resistance of hTspan1 to be silenced by rTspan1-shRNA was controlled by immunoblotting and immunofluorescence of PC12-transfected cells (Fig. 2e, f).

Expression of Tspan1 during DRG development

The role of Tspan1 in the central and peripheral nervous system development is still completely unknown. To start addressing this, the expression of *Tspan1* mRNA was analyzed by real-time PCR in rat DRG tissue at different developmental stages. A developmental increase in *Tspan1* mRNA expression was detected between E15.5 and E17.5 (Fig. 3a), a period in which DRG sensory neurons receive target-derived NGF [9].

To explore whether Tspan1 could play a role in NGF/TrkA function in vivo, we analyzed the expression pattern of Tspan1 and TrkA in tissue sections of DRGs by immunofluorescence using specific antibodies (Fig. 3b). Quantitative analysis revealed that from E15.5 to E17.5, the expression of Tspan1 is localized in ≈40–50% of TrkA-positive neurons (Fig. 3c). In addition, more than 80% of the Tspan1-positive cells also express TrkA (Fig. 3d), thereby suggesting that Tspan1 might contribute to the biological response triggered by NGF in DRG neurons in vivo.

Primary cultures of dissociated DRG neurons obtained from E15 rats and maintained in the presence of NGF for 48 h, were evaluated by immunofluorescence using anti-Tspan1 and anti-TrkA antibodies. In agreement with the in vivo data, the staining revealed a high co-expression of Tspan1 and TrkA in DRG-cultured neurons (Fig. 3e). Antibody specificity was controlled by immunoblot and immunofluorescence of cells transfected with *Tspan1*-shRNA (Supplementary Fig. 1a, b) and by immunofluorescence of

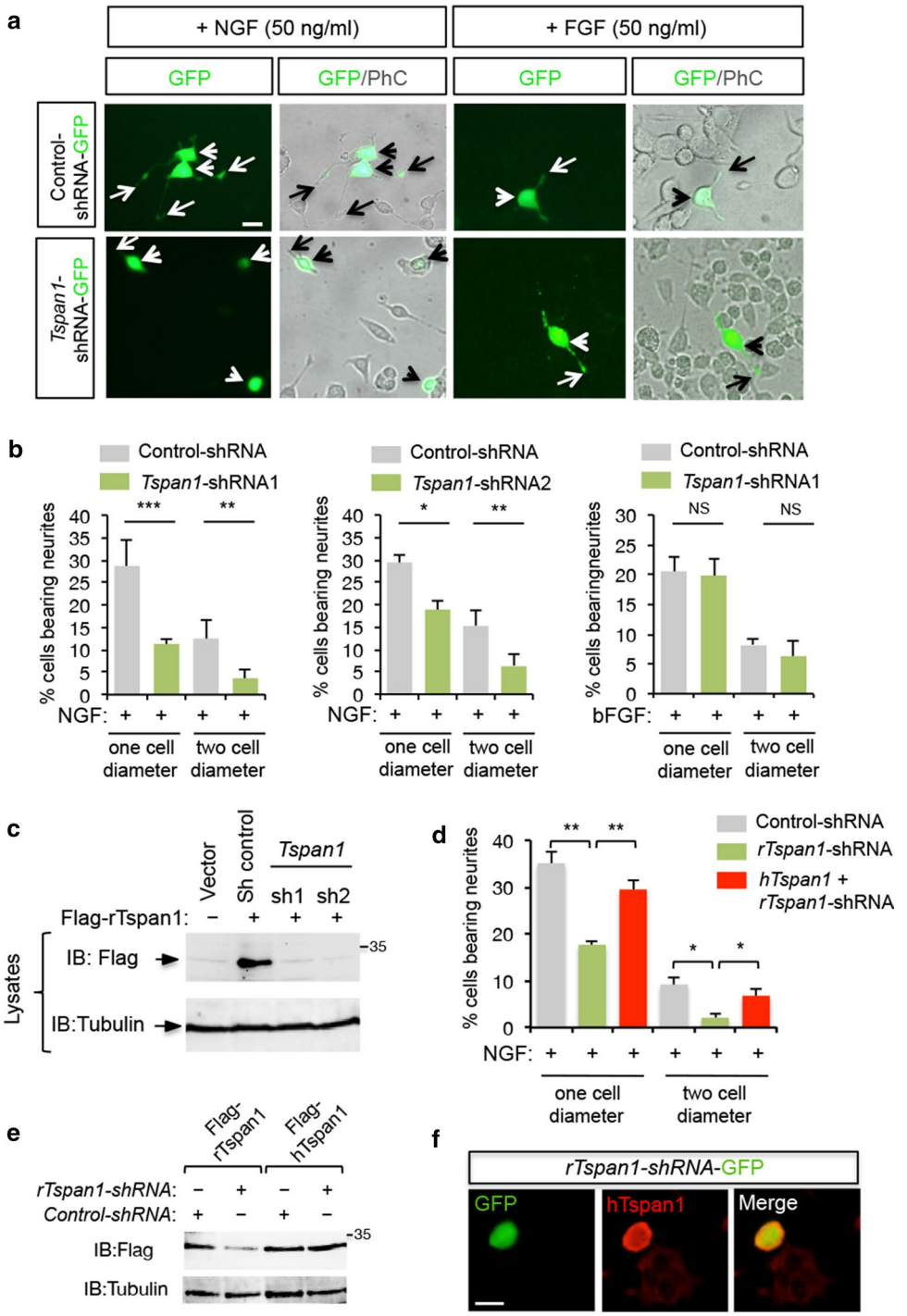

PC12 cells overexpressing myc-tagged rat Tspan1 (Supplementary Fig. 1c).

The expression of Tspan1 in TrkA-positive sensory neurons, together with its upregulation during the period of NGF-dependent axonal growth and target tissue innervation, suggested that Tspan1 could mediate in vivo effects of NGF during embryonic development.

Tspan1 is involved in axonal growth of DRG sensory neurons in response to NGF

The results obtained in PC12 cells lead us to examine the biological significance of Tspan1 as a mediator of NGF signaling in primary sensory neurons. For such purpose, we introduced *Tspan1*-shRNA construct expressing GFP into sensory neurons isolated from E15 DRG. At this developmental stage, the majority of the DRG neurons express high

◂**Fig. 2** Knockdown of Tspan1 inhibits PC12 cell differentiation in response to NGF. **a** Photomicrographs show PC12 cell transfected with control-shRNA-GFP or *Tspan1*-shRNA-GFP constructs. After 48 h of NGF (50 ng/ml) or bFGF (50 ng/ml) treatment, the cells were fixed and analyzed. Arrowheads indicate neuronal cell bodies (CBs) and arrows denote neurite tips. PhC, Phase Contrast. Scale bar, 15 µm. **b** Quantification of the relative number of GFP-positive neurite-bearing PC12 cells longer than one or two CB diameters in the different experimental groups after 48 h of NGF or bFGF treatment. The results are shown as mean ± SD of three independent experiments $*p \leq 0.01$; $**p \leq 0.005$; and $***p \leq 0.001$ by Student's *t* test. **c** Tspan1 protein levels were analyzed by immunoblotting of Cos cells co-transfected with Flag-Tspan1 and either control-shRNA or *Tspan1*-shRNA constructs. Tubulin is shown as loading control. Two different *Tspan1*-shRNAs (sh1 and sh2) have been tested in these assays. **d** shRNA-resistant human Tspan1 (hTspan1) rescues the effect of rat *Tspan1*-shRNA on NGF-promoted neurite outgrowth. Quantification of the % of GFP-positive neurite-bearing PC12 cells longer than one or two CB diameters in the different experimental groups after 24 h of NGF treatment. The results are shown as mean ± SD of three independent experiments. $*p \leq 0.05$ and $**p \leq 0.01$ by one-way ANOVA followed by Student–Newman–Keuls' multiple comparisons test. **e** Representative immunoblot analysis of Flag-tagged Tspan1 with anti-Flag antibody following transfection of Cos cells with control or rTspan1-shRNA constructs in combination with Flag-ratTspan1 or an shRNA-resistant Flag-hTspan1. Tubulin is shown as loading control. **f** Tspan1 immunofluorescence (red) of rat PC12 cells co-transfected with human Tspan1 (hTspan1) together with rTspan1-shRNA-GFP. Note that the anti-hTspan1 immunolabeling is clearly detected in GFP-positive cells expressing a rat-specific Tspan1-shRNA, thereby showing that hTspan1 is resistant to the shRNAs used

levels of TrkA and respond to the neurotrophin NGF. After transfection, the cells were maintained in the presence of NGF for 36 h, fixed, and analyzed for neuronal differentiation. In agreement with the results obtained in PC12 cells, the neurite outgrowth stimulated by NGF was significantly reduced in DRG neurons transfected with *Tspan1* shRNA (Fig. 3f, g).

To discard the possibility that the effect seen with *Tspan1*-shRNA was due to apoptosis, the cultures were treated with the apoptotic inhibitor Z-VAD-FMK (50 nM) and the morphology of the nuclei was additionally assessed using the nuclear staining DAPI. A similar survival was observed between control and *Tspan1*-shRNA-transfected neurons. This result indicates that the effect of Tspan1 in sensory neuron axonal growth is independent of neuronal survival (Fig. 3h). Thus, our findings demonstrate that Tspan1 is required for sensory neuron axonal growth in response to NGF.

Tspan1 facilitates NGF-mediated activation of TrkA receptor tyrosine kinase and downstream signaling pathways

To evaluate whether Tspan1 could promote NGF signaling, we transiently transfected PC12 cells with either control plasmid or Myc-DDK-Tspan1 construct. Transfected cells were serum-starved, stimulated with NGF for 15 min, and fixed. Activation of TrkA was evaluated by immunofluorescence [8] using a specific anti-phospho TrkA (Tyr490) antibody. In these assays, the overexpression of Tspan1 promotes a significant increase in NGF-induced TrkA phosphorylation compared to control transfected cells (Fig. 4a, b). In addition, we examined biochemical events associated with TrkA receptor signaling by immunoblotting. In these experiments, parental PC12 and stable transfected PC12 cells overexpressing Tspan1 (PC12-Tspan1 cells, clon T7) were serum-starved and treated with or without NGF for 15 min. The levels of TrkA and Erk1/2 activation were evaluated in cell extracts by immunoblotting (IB) with anti-phospho TrkA and anti-phospho Erk1/2 antibodies, respectively. In agreement with the activation of TrkA observed by immunofluorescence (Fig. 4a, b), the stable expression of Flag-Tspan1 (clon T7) showed a robust increase in TrkA phosphorylation and Erk activation compared to parental PC12 cells (Supplementary Fig. 2).

The promotion of NGF/TrkA signaling observed in PC12 cells overexpressing Tspan1 prompted us to examine whether the downregulation of Tspan1 can attenuate TrkA and Erk2/MAPK activation in response to NGF. To perform this, we co-expressed full-length HA-TrkA or HA-Erk2 plasmids together with either control-shRNA-GFP or *Tspan1*-shRNA-GFP construct. In these experiments, transfected cells were serum-starved and treated with or without NGF for 15 min. The levels of HA-TrkA and HA-Erk2 activation were evaluated by immunoprecipitation followed by immunoblotting with anti-phospho-specific antibodies. In agreement with the results obtained by gain of function assays, a significant ligand-dependent inhibition of TrkA tyrosine phosphorylation and Erk2 activation were observed in PC12 cells transfected with *Tspan1*-shRNA (Fig. 4c–f). Together, our findings indicate that Tspan1 facilitates TrkA signaling and physiological responses to NGF.

Tspan1 interacts with the immature form of TrkA and regulates its post-biosynthetic trafficking

To obtain additional insight into the mechanisms underlying the role of Tspan1 in NGF-mediated TrkA signaling, we conducted a series of biochemical and immunofluorescence assays. Initially, we examined by immunofluorescence the cellular localization of endogenous TrkA and Myc-Tspan1 in PC12 cells. Our findings indicate that TrkA and Myc-Tspan1 are highly co-localized together with the ER marker Calnexin (CNX) (Fig. 5a), indicating that Tspan1 may form a molecular complex with TrkA in this compartment. Perinuclear co-localization between endogenous TrkA and Tspan1 was also detected in PC12 cells by immunofluorescence (Fig. 5b). To address this possibility, HEK-293 cells were transfected with expression vectors encoding

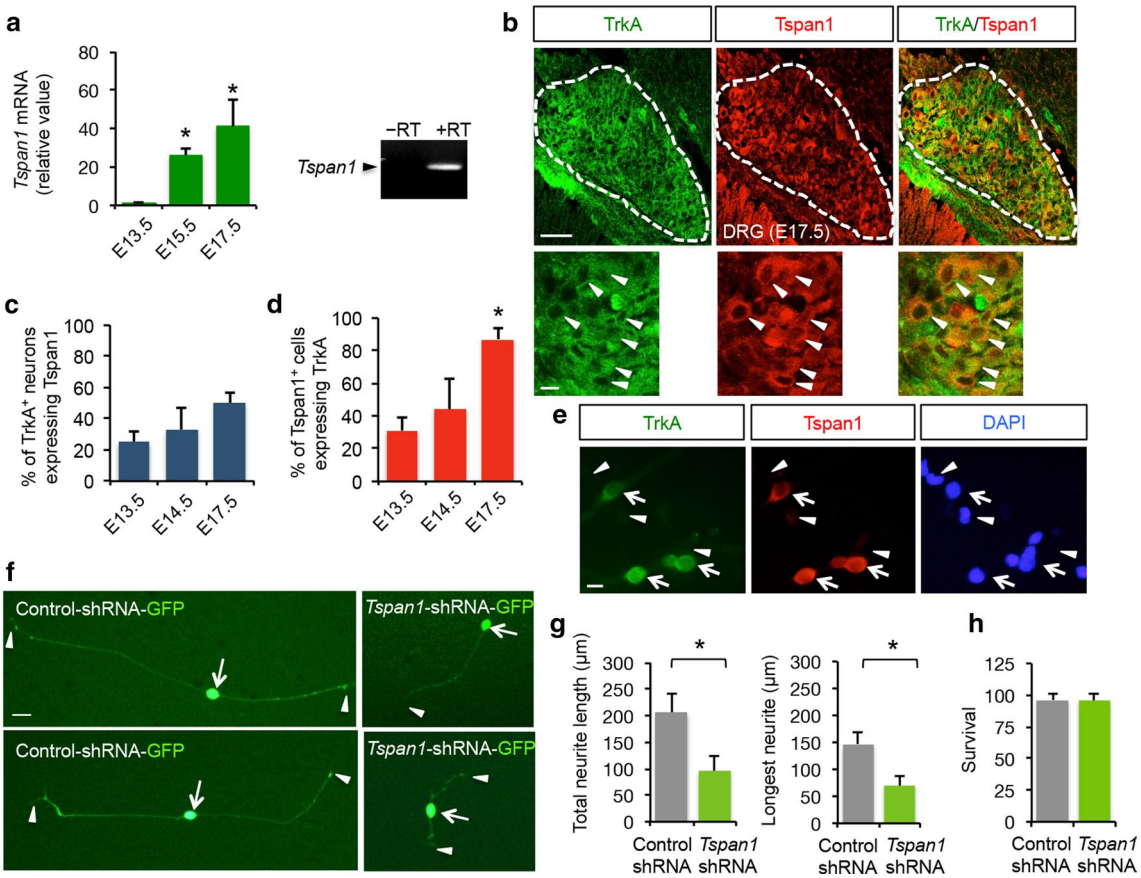

Fig. 3 Tspan1 is expressed in TrkA-positive DRG sensory neurons and its knockdown restricts NGF-induced axonal growth. **a** Quantitative analysis of the developmental expression of *Tspan1* mRNA by real-time PCR in rat DRG ganglia at the indicated embryonic stages. Expression was normalized to the housekeeping gene *Tbp* and values are relative to the expression at E13.5. Right, *Tspan1* mRNA expression by PCR in DRG. Control sample without reverse transcriptase (-RT) was included. $*p \leq 0.05$ vs. E13.5 by one-way ANOVA. **b** Immunofluorescence of TrkA and Tspan1 in E17.5 rat DRG sections. High magnification images are also shown. Arrowheads indicate cells showing Tspan1-TrkA co-expression. Scale bar, 50 μm (upper panel) and 10 μm (lower panel). **c** and **d** Quantitative analysis of developmental co-expression of Tspan1 with TrkA in lumbar DRG sections. **c** Averages are expressed as percent (%) of TrkA-positive neurons expressing Tspan1 and **d** Averages are expressed as percent of Tspan1-positive cells expressing TrkA. $*p \leq 0.05$ vs. E13.5 and E14.5 by one-way ANOVA followed by Student–Newman–Keuls' multiple comparisons test. **e** Localization by immunofluorescence of TrkA (green) and Tspan1 (red) in DRG-dissociated neurons. Arrows indicate cells showing Tspan1-TrkA co-expression. Arrowheads indicate cells negative for TrkA and Tspan1. Scale bar, 15 μm. **f** Dissociated DRG neurons transfected with control-shRNA-GFP or *Tspan1*-shRNA-GFP constructs, cultured in the presence of the apoptosis inhibitor Z-VAD-FMK (50 nM), and maintained in the presence of NGF (50 ng/ml). After 36 h in culture, neurons were fixed and analyzed. Scale bar, 20 μm. Arrows indicate cell bodies and arrowheads indicate neurite tips. **g** Histograms show the inhibition of neurite outgrowth in DRG neurons by knockdown of *Tspan1* expression. The total neurite length and the length of the longest neurite were evaluated. Results are shown as the average ± SD of three independent experiments $*p \leq 0.05$ by Student's *t* test. **h** Histogram showing the survival of DRG neurons transfected with control-shRNA-GFP or *Tspan1*-shRNA-GFP. Neuronal survival was evaluated using DAPI for the nuclear staining. GFP-positive neurons containing fragmented or condensed nuclear staining were scored as apoptotic cells. The results are expressed as averages ± SD of three independent experiments

HA-tagged TrkA in the absence or in the presence of Myc-Flag-Tspan1, and then, Tspan1 was immunoprecipitated with anti-Flag antibodies. As shown in Fig. 5c, TrkA was specifically co-immunoprecipitated with anti-Flag antibodies only from cells co-expressing both constructs, but not from cells transfected with control or TrkA plasmid alone. Interestingly, our findings show that Tspan1 interacts with the immature form of TrkA (110 kDa) that has not completed golgi-mediated processing of high-mannose *N*-glycans, but not with the upper mature band expressed at the cell surface (140 kDa) [36]. To confirm this interaction, we carried out the same type of experimental design but using a TrkA mutant (L213P) that only generates the immature protein band of 110 kDa, because this variant of TrkA is retained in the ER and does not traffic correctly towards the plasma membrane [31]. This further analysis using the TrkA-L213P clearly demonstrates that Tspan1 interacts in the ER with the 110 kDa-intracellular form of TrkA (Fig. 5c).

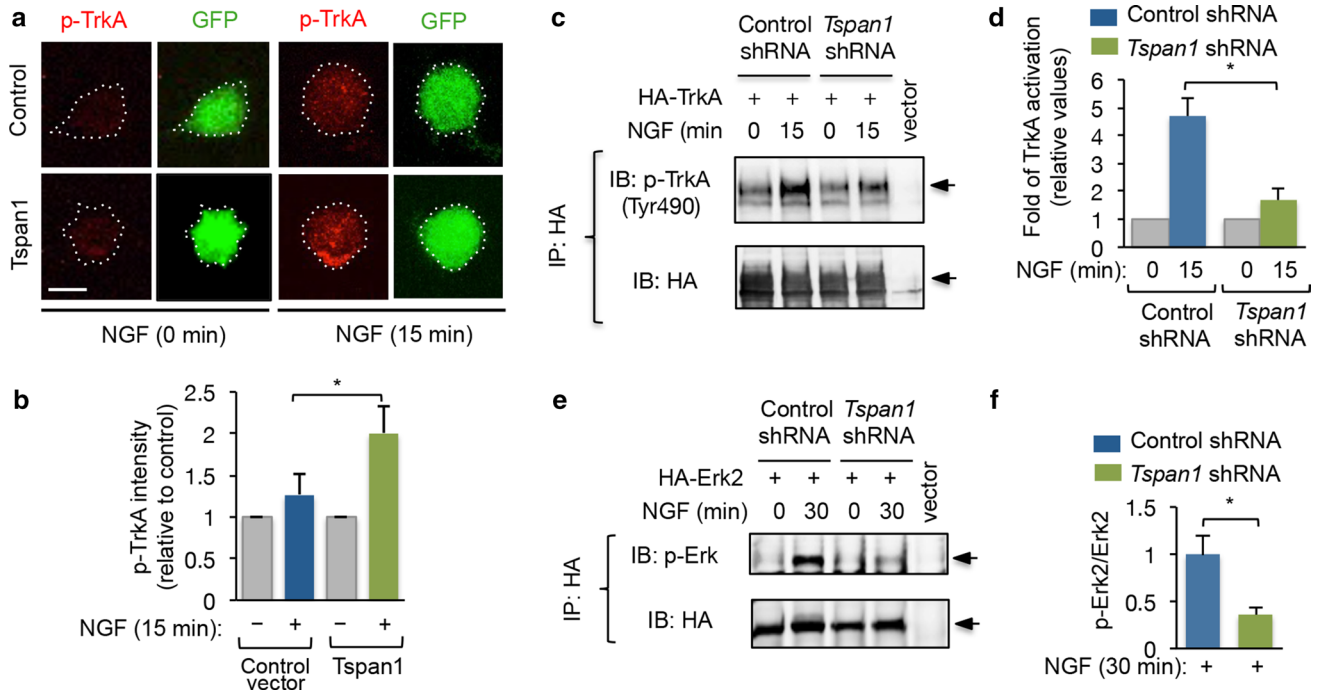

Fig. 4 Tspan1 promotes NGF-induced TrkA signaling. **a** Photomicrographs show PC12 cells transfected with control vector or Myc-Tspan1 (Tspan1) construct together with a GFP plasmid. After 48 h the cells were serum-starved, then treated or not with NGF (25 ng/ml) for 15 min, and fixed. Activation of TrkA was assessed by immunofluorescence of phospho TrkA (p-TrkA) on GFP-positive cells. Scale bar, 10 µm. **b** Quantitative analysis of p-TrkA activation expressed as average ± SD of three independent assays. *$p \leq 0.05$ by Student's *t* test. **c** TrkA phosphorylation in PC12 cells co-transfected with either control-shRNA or *Tspan1*-shRNA constructs together with HA-tagged TrkA vector. Cells were treated with NGF (50 ng/ml) as indicated. Total lysates were immunoprecipitated (IP) with anti-HA antibodies followed by immunoblot (IB) with antibodies against phospho-Tyr 490 of TrkA (p-TrkA). Reprobing of the same blot with anti-HA antibodies is shown. **d** Quantification of TrkA phosphorylation expressed as fold of TrkA activation relative to untreated cells. Results are presented as averages ± SD from three independent experiments. *$p \leq 0.005$ by Student's *t* test. **e** Erk2 activation in cell extracts prepared from PC12 cells co-transfected with either control-shRNA or *Tspan1*-shRNA constructs together with HA-tagged Erk2 vector. Cells were treated with NGF (50 ng/ml) as indicated. Reprobing of the same blot with anti-βIII-tubulin is shown. **f** The graph bar shows the quantification of Erk2 phosphorylation. Results are presented as average ± SD from three independent experiments. *$p \leq 0.005$ by Student's *t* test

To determine whether this interaction between Tspan1 and TrkA occurs when these proteins are expressed at physiological levels, Tspan1 was immunoprecipitated from tissue extracts prepared from rat DRG. This assay clearly shows that the immature form of TrkA can be specifically co-immunoprecipitated with Tspan1, but not with control antibodies (Fig. 5d), confirming that Tspan1 and immature TrkA specifically associate in vivo. Notably, the reprobing with anti-CNX of the same filters previously tested with anti-HA or anti-TrkA reveals that Tspan1 also interacts with the lectin chaperone CNX (Fig. 5c, d). Together, these assays support that the association between Tspan1 and immature TrkA occur in the ER, and suggest that Tspan1 might be involved in the post-synthetic trafficking of TrkA, by promoting its early association with CNX.

Previous studies indicated that in addition to their purely structural function as membrane organizers, tetraspanins also regulate various aspects of trafficking and biosynthetic processing of associated proteins [37]. Thus, this evidence prompted us to examine whether Tspan1 could affect the abundance of TrkA on the cell surface. To this end, we performed two different complementary approaches. First, PC12 cells were transfected with either control-shRNA-GFP or *Tspan1*-shRNA-GFP construct. After 72 h, the cells were fixed and the TrkA surface levels were evaluated by immunofluorescence with anti-TrkA extracellular domain ($TrkA^{ECD}$) antibodies on non-permeabilized cells. Only receptors placed on the cell surface were labeled with the anti-$TrkA^{ECD}$ antibodies (see Supplementary Fig. 3). Using this analysis, we found that knockdown of *Tspan1* in PC12 cells causes a significant reduction (≅33%) in the cell-surface levels of TrkA (Fig. 6a, b). This biological effect was rescued using an shRNA-resistant hTspan1 construct, which was sufficient to reverse the reduced TrkA surface levels observed upon knockdown of rTspan1 (Supplementary Fig. 4a, b).

To assess the specificity of Tspan1 on TrkA trafficking to the cell surface, we evaluated whether Tspan1 could affect

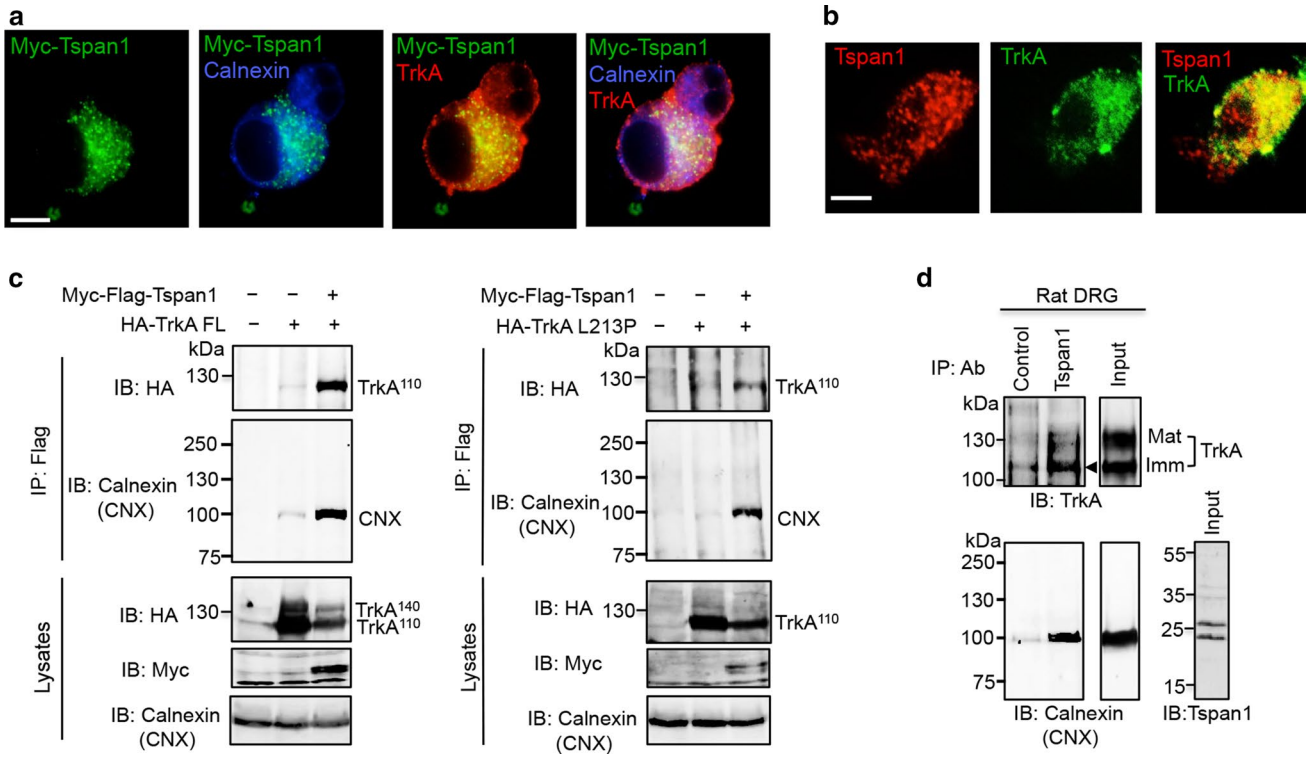

Fig. 5 Tspan1 interacts with the immature form of TrkA receptor in the ER. **a** Representative confocal immunofluorescence of PC12 cells transfected with Myc-Tspan1. The images show co-localization between Myc-Tspan1 (green) with endogenous TrkA (red) and the ER marker Calnexin (blue). Scale bar, 5 µm. **b** Confocal immunofluorescence images showing co-localization between endogenous Tspan1 (red) and TrkA (green) in PC12 cells. Scale bar, 5 µm. **c** Co-immunoprecipitation between Myc-Flag-tagged Tspan1 and HA-TrkA (left) or HA-TrkA L213P (right) overexpressed in HEK-293 cells. Cell extracts were analyzed by immunoprecipitation (IP) with anti-Flag antibody followed by immunoblot (IB) with antibodies against HA. The same blots were reprobed with anti-CNX antibodies. Expression of HA-TrkA, Myc-Flag-Tspan1 and endogenous CNX in cell lysates is also shown. **d** Co-immunoprecipitation between endogenous Tspan1 and TrkA from E17.5 rat DRGs. Tissue extracts were analyzed by IP with anti-Tspan1 antibody, followed by IB with anti-TrkA. The same blot was also reprobed with anti-CNX. One aliquot of the starting material (Input) is included. Expression of TrkA (Mat: mature and Imm: immature forms) are indicated. Arrowhead indicates the band of immature TrkA associated with Tspan1. Similar results were obtained in three independent assays

the surface levels of the NGF low affinity receptor p75NTR. We performed a parallel experiment using anti-p75NTR^{ECD} antibodies, but we could not observe changes in the membrane levels of this receptor, indicating that the effect of Tspan1 is specific on TrkA (Fig. 6c, d). Furthermore, DRG sensory neurons transfected with *Tspan1*-shRNA-GFP also showed a significant decrease (≅32%) in the surface levels of TrkA compared to control transfected neurons, supporting a physiological role of Tspan1 in the intracellular trafficking of TrkA (Fig. 6e, f).

Next, we performed a surface biotinylation assay on parental and PC12 cells transfected with Tspan1-shRNA (*shTspan1*-PC12 cells). Biotinylated TrkA was detected by TrkA immunoprecipitation followed by immunoblotting with anti-biotin. We found that knockdown of *Tspan1* substantially reduces the levels of biotinylated TrkA compared to parental cells. Intriguingly, the expression of the mature form of TrkA (140 kDa) detected by immunoblot on the total cell lysates was markedly reduced, and accompanied the low level of biotinylated TrkA detected in *shTspan1*-PC12 cells (Fig. 6g). Further immunoblot comparison of mature and immature TrkA levels between parental and *shTspan1* PC12 cell lysates revealed a significant decrease in the mature, but not in the immature form of TrkA upon knockdown of Tspan1 (Fig. 6h, i). Semi-quantitative RT-PCR indicates that the levels of *TrkA* mRNA expression were not affected by downregulating Tspan1 (Fig. 6j). Therefore, our findings demonstrate that Tspan1 is required for proper biosynthetic trafficking of TrkA to the plasma membrane and suggest that knockdown of *Tspan1* reduces the surface levels of TrkA by promoting its sorting towards degradative pathways.

Knockdown of Tspan1 conducts TrkA to the autophagic/lysosomal degradation pathway

Our previous findings showing that Tspan1 interacts with the inmature form of TrkA in the ER (Fig. 5) and that downregulation of Tspan1 drastically reduced the levels of

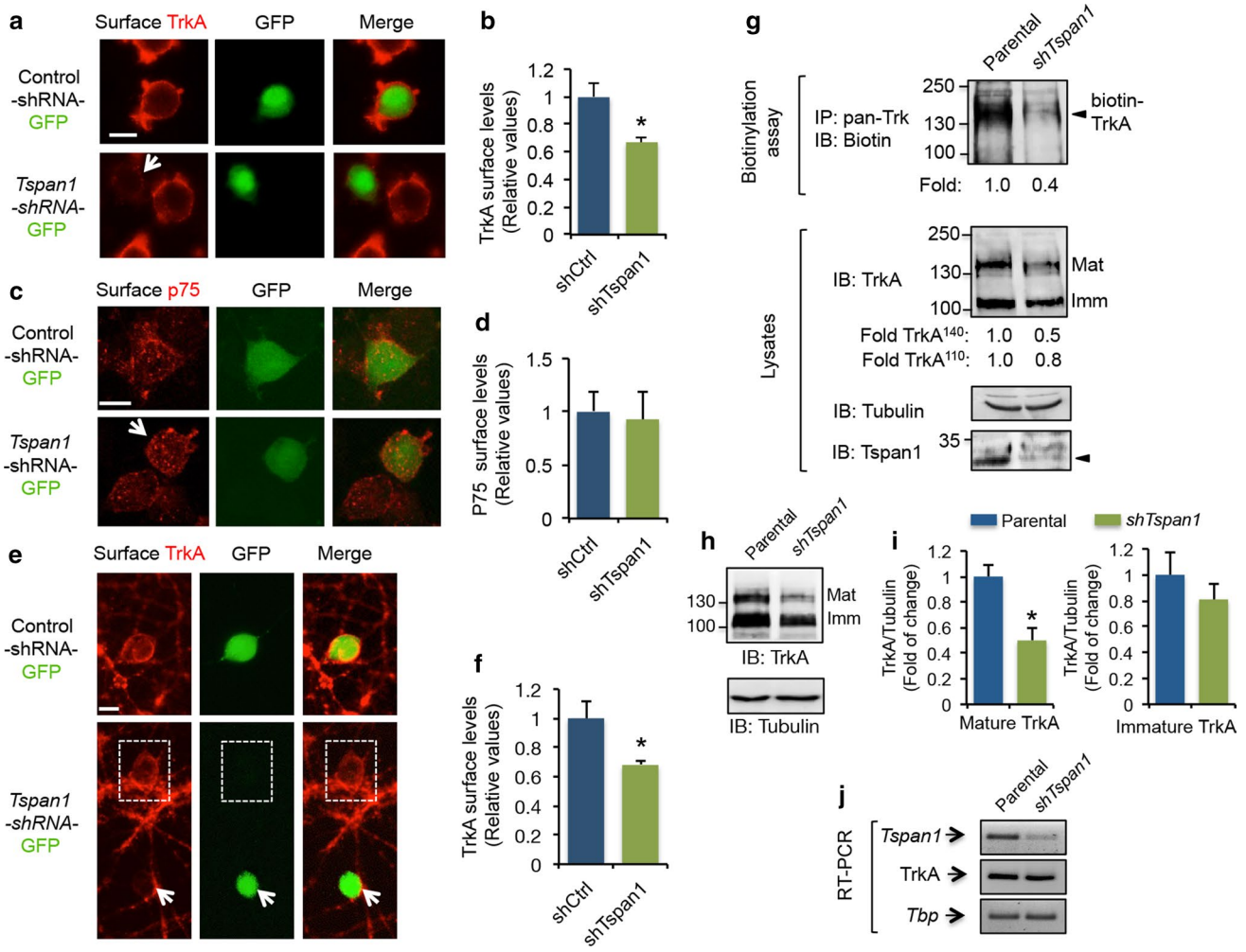

Fig. 6 Tspan1 downregulation reduces cell-surface expression of TrkA, but not p75NTR in PC12 cells. **a** Immunofluorescence assay to quantify TrkA cell-surface expression in PC12 cells transfected with either control-shRNA-GFP (shCtrl) or *Tspan1*-shRNA-GFP (shTspan1) constructs. TrkA immunofluorescence was performed by staining non-permeabilized cells with an anti-TrkA^{ECD} antibody. Arrow shows an shTspan1 transfected cell. Scale bar, 10 µm. **b** Quantification of TrkA surface levels relative to control-shRNA-transfected cells. The results are shown as means ± SD of three independent experiments. *$p \leq 0.05$ by Student's *t* test. **c** Immunofluorescence assay to quantify p75NTR cell-surface expression in PC12 cells transfected with either control-shRNA-GFP or *Tspan1*-shRNA-GFP constructs. p75NTR immunofluorescence was performed by staining non-permeabilized cells with an anti-p75NTR^{ECD} antibody. Arrow shows a *Tspan1*-shRNA-transfected cell. Scale bar, 10 µm. **d** Quantification of p75NTR surface levels relative to control-shRNA-transfected cells. The results are shown as means ± SD of three independent experiments. **e** Immunofluorescence assay to quantify TrkA cell-surface expression in rat DRG sensory neurons transfected with either control-shRNA-GFP (shCtrl) or *Tspan1*-shRNA-GFP (shTspan1) constructs. TrkA immunofluorescence was performed by staining non-permeabilized cells with an anti-TrkA^{ECD} antibody. Arrow shows an shTspan1 transfected neuron. Dotted square shows TrkA surface labeling of an shRNA non-transfected neuron. Scale bar, 10 µm. **f** Quantification of TrkA surface levels relative to control-shRNA-transfected cells. The results are shown as means ± SD of three independent experiments. *$p \leq 0.05$ by Student's *t* test. **g** Representative immunoblot of biotinylated TrkA in parental and PC12 cells expressing *Tspan1*-shRNA. Cell-surface levels of TrkA were evaluated using a surface biotinylation assay. Biotinylated TrkA was detected by Trk immunoprecipitation and probing with an anti-biotin antibody. Fold change of biotinylated TrkA relative to βIII-tubulin is indicated. Immunoblots showing the expression levels of TrkA, βIII-Tubulin and Tspan1 in parental and *shTspan1* PC12 cell lysates are also shown. Fold change of mature and immature (Imm) TrkA relative to βIII-tubulin is indicated. Similar results were obtained in three independent assays. **h** Representative immunoblots of TrkA and βIII-Tubulin in parental and *shTspan1* PC12 cell lysates. **i** Quantification of mature and immature TrkA levels in parental and *shTspan1* PC12 cell lysates. Data are normalized by βIII-tubulin and expressed as relative values. Results are presented as means ± SD from three independent experiments. *$p \leq 0.05$ by Student's *t* test. **j** Semi-quantitative RT-PCR of *Tspan1*, *TrkA* mRNA, and the housekeeping gene *Tbp*. Note the substantial decrease in *Tspan1* mRNA expression observed in *Tspan1*-shRNA-transfected cells compared to parental ones

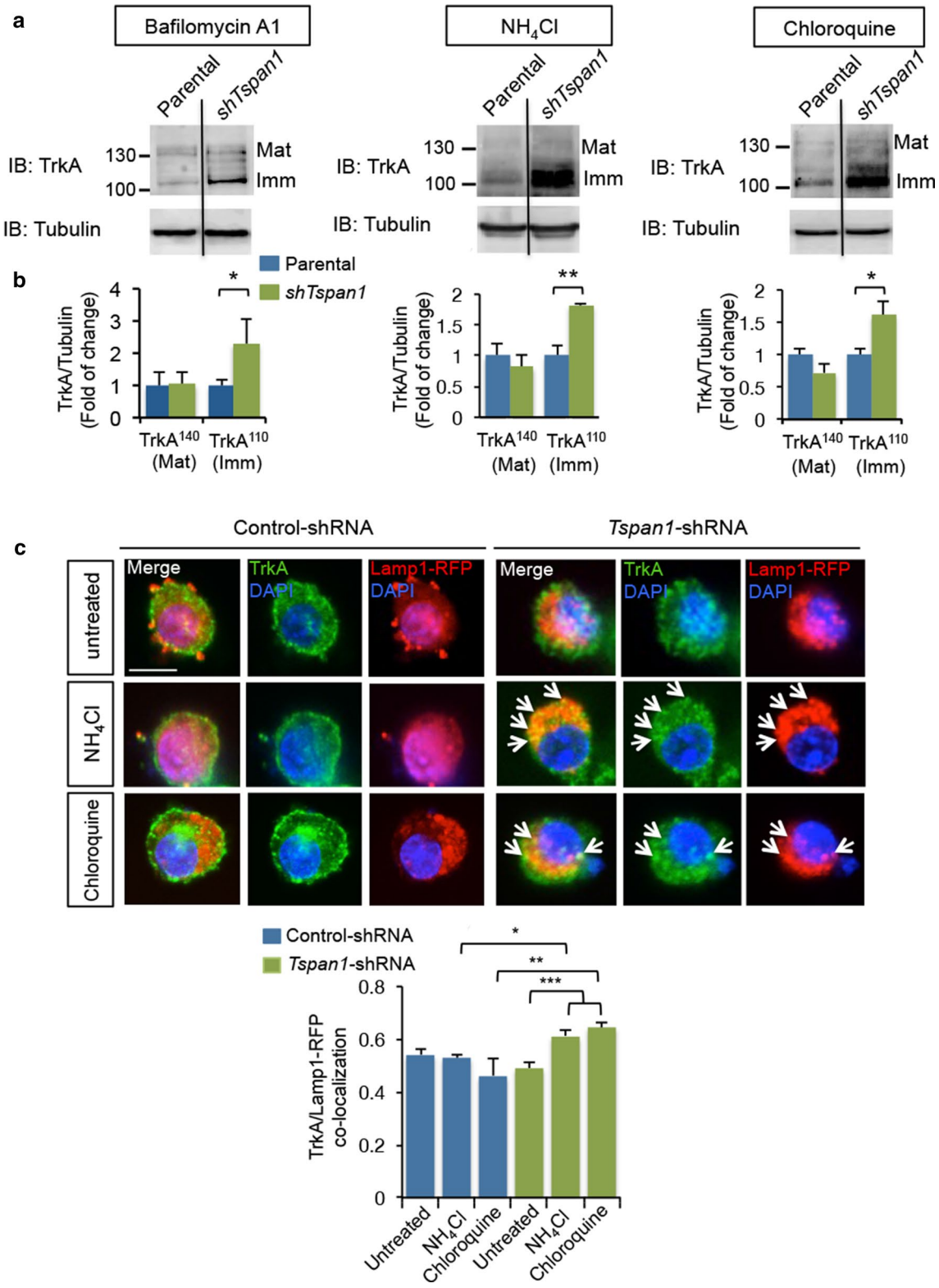

TrkA (Fig. 6h, i) prompted us to examine whether Tspan1 is involved in TrkA stability and degradation. We focused on the autophagic/lysosomal pathway, because this route has been linked to the biosynthetic degradation of TrkA [31].

We tested the degradation pathways of TrkA using inhibitors of the autophagic/lysosomal pathways such as Chloroquine and ammonium chloride (NH_4Cl), two lysosomotropic agents that prevents lysosomal acidification and Bafilomycin

◂**Fig. 7** Knockdown of Tspan1 conducts TrkA to the autophagic/lysosomal pathway. **a** Immunoblots showing mature and immature (Imm) TrkA expression levels in cell extracts from parental and *Tspan1*-shRNA (*shTspan1*) PC12 cells treated with Bafilomycin A1, NH_4Cl, or Chloroquine as indicated in materials and methods. Reprobing of the same blot with anti-βIII-tubulin is shown. **b** Quantification of mature and immature TrkA levels normalized by βIII-tubulin. Results are presented as means ± SD from three independent experiments. $*p \leq 0.05$ and $**p \leq 0.01$ by Student's *t* test. **c** Confocal images showing co-localization between TrkA immunofluorescence (green) and Lamp1-RFP (red). PC12 cells were co-transfected with either control-shRNA-GFP or *Tspan1*-shRNA-GFP together with Lamp1-RFP and treated or not with NH_4Cl or Chloroquine as indicated in materials and methods. Arrows denote co-localization between TrkA and Lamp1-RFP. Scale bar, 10 µm. **d** Pearson's coefficient to assess the co-localization between TrkA (Green) and Lamp1-RFP of the assay described in (**c**). The results are shown as mean ± SD of $n = 3$ independent experiments. $*p < 0.05$; $**p < 0.01$ and $***p < 0.001$ by one-way ANOVA followed by Student–Newman–Keuls' multiple comparisons test

A1, an inhibitor of the late phase of the autophagy that inhibits the fusion between autophagosomes and lysosomes.

Parental and *shTspan1*-PC12 cells were treated with these different inhibitors and the levels of mature and immature forms of TrkA were determined by immunoblotting. From these assays, we observed that the treatment with these lysosomal inhibitors caused a significant accumulation of immature forms of TrkA (110 kDa) in PC12 cells expressing *Tspan1*-shRNA, indicating that immature TrkA becomes resistant to degradation in the presence of these inhibitors (Fig. 7a, b). Altogether these findings indicate that the downregulation of Tspan1 quickly drives immature forms of TrkA towards degradation by the autophagic/lysosomal pathway. Changes in lysosomal acidity were controlled using LysoTracker Green. Compared to control untreated cells, a faint staining of LysoTracker Green was observed in PC12 cells pretreated with Chloroquine and NH_4Cl, indicating that these lysosomotropic drugs disrupted lysosomal acidity (Supplementary Fig. 5).

Then, we decided to further examine whether *Tspan1* knockdown affects the TrkA localization in lysosomes of cells treated in the absence or in the presence of the lysosomal inhibitors Chloroquine or NH_4Cl. For these assays, PC12 cells were co-transfected with either control-shRNA-GFP or *Tspan1*-shRNA-GFP together with a plasmid encoding for the lysosomal marker Lamp1-RFP and the co-localization of these molecules was analyzed. We calculated the Pearson´s coefficient between TrkA and Lamp1-RFP. In agreement with our previous results, a significant increase in TrkA/Lamp1 co-localization was only observed in those cells transfected with *Tspan1*-shRNA and treated with the lysosomal inhibitors, Chloroquine or NH_4Cl, indicating that in these experimental conditions, downregulation of Tspan1 leads to the accumulation of TrkA into lysosomal vesicles (Fig. 7c, d).

Finally, we decided to further explore how Tspan1 affects TrkA trafficking and degradation. Since sensitivity to digestion with trypsin is indicative of protein misfolding, we performed a trypsin sensitivity assay to study the folding status of the immature TrkA. For this, we incubated both parental and *shTspan1* cell lysates with increasing concentrations of trypsin and evaluated the degradation pattern of the immature band of TrkA by immunoblotting. We observed that downregulation of Tspan1 affects the accessibility of the protease to digest the immature TrkA, suggesting that Tspan1 may regulate the folding of TrkA at the ER (Fig. 8a, b).

Protein misfolding may induce the exposition of hydrophobic residues to the protein surface promoting protein aggregation. The higher resistance to trypsin degradation detected in *shTspan1* cell extracts also suggests that Tspan1 could be affecting the folding and thereby the aggregation state of TrkA in the ER. To explore if the changes observed in trypsin-mediated immature TrkA degradation could be accompanied by protein aggregation, parental and *shTspan1* cells were lysed with buffer containing the detergent Triton X-100, and after centrifugation, the pellet was treated with SDS-PAGE buffer containing SDS and β-Mercaptoethanol. Result from this experiment shows that downregulation of Tspan1 promotes a substantial increase of the immature form of TrkA in the pellet, suggesting its possible aggregation in the ER (Fig. 8c). Together, these assays suggest that Tspan1 regulate the biosynthetic trafficking of TrkA by controlling the folding/aggregation state of the newly synthesized TrkA at the ER.

Discussion

Although Trk receptors are expressed in specific subsets of peripheral and central neurons, they cannot by themselves explain the complex pattern of neuronal connectivity that characterizes the vertebrate nervous system. Recent studies have established that neurotrophin signaling is tightly modulated through the coordinated action of many different endogenous regulators that restrict or potentiate signal propagation in spatially and temporally controlled manners [38]. Genetically modified mouse models have demonstrated that Trk activity needs to be modulated by different proteins to achieve cell-type specific responses to their cognate ligands during circuit development [13]. Particular attention was also given to the mechanisms that control cell surface targeting of TrkA, because this event is crucial in determining cellular responsiveness to NGF [39]. In this study, we establish a novel homeostatic mechanism to control biosynthetic trafficking and degradation of TrkA, regardless of the presence of NGF. In particular, our findings establish that knockdown of *Tspan1* promotes a preferential guidance of

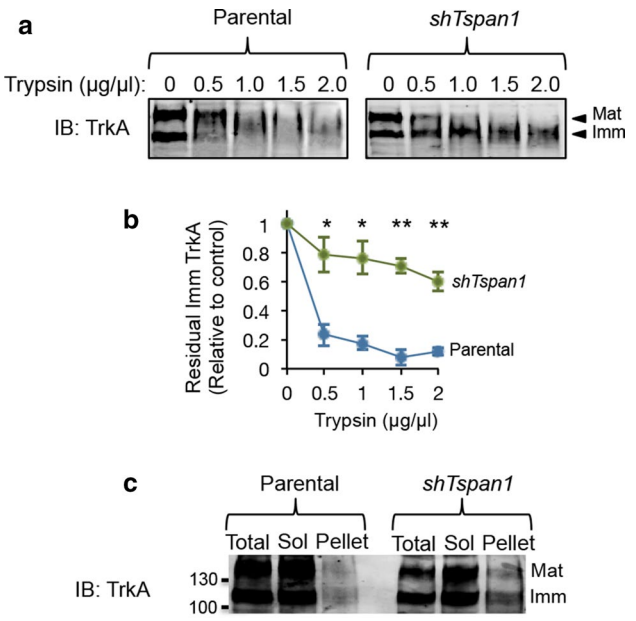

Fig. 8 Knockdown of Tspan1 induces immature TrkA protein misfolding/aggregation. **a** Representative TrkA immunoblot showing trypsin digestion of parental and *shTspan1* PC12 cell extracts. Samples were incubated with the indicated concentrations of trypsin during 10 min on ice. Digestions were stopped by adding sample buffer, and boiled and analyzed by TrkA immunoblotting. Mature and Immature (Imm) forms of TrkA are indicated. **b** Quantification of residual immature (Imm) TrkA protein levels in parental and shTspan1 PC12 cell extracts treated with different concentrations of trypsin. The results are shown as mean ± SEM of $n = 3$ independent experiments. $^{*}p < 0.05$; $^{**}p < 0.005$ by Student's t test. **c** Analysis of TrkA protein solubility from parental and *shTspan1* cell extracts prepared in lysis buffer supplemented with the non-ionic detergent Triton X-100. Insoluble TrkA was pulled down by centrifugation at 20,000×*g* for 40 min. Aliquots of total, soluble, and pellet fractions were analyzed for TrkA immunoblotting

TrkA molecules towards the autophagic-lysosomal pathway instead of its biosynthetic trafficking to the plasma membrane. Our data also indicate that Tspan1 is a physiological TrkA receptor interactor able to associate in the ER with the immature form of TrkA to control the biosynthetic trafficking and degradation of this neurotrophin receptor (Fig. 9). In line with these findings, previous studies have revealed a critical role of Tspans in the regulation of ADAM10 metalloprotease exit from the endoplasmic reticulum and its subsequent trafficking to the plasma membrane. Further evidence demonstrated that Tspans can also regulate the function of the ADAM10 partner proteins by acting on their membrane compartmentalization [40–42].

Our finding indicating that the knockdown of *Tspan1* restricts axonal growth of DRG sensory neurons in response to NGF suggests that Tspan1 could be involved in peripheral circuit development and axonal regeneration following acute nerve injury. Neuronal responsiveness to target-derived NGF requires the precise axonal targeting of newly synthesized TrkA receptors. Recent studies indicated that internalization and retrograde transport of TrkA receptors from axon terminals to cell bodies must be balanced by the anterograde delivery of newly synthesized TrkA receptors or by transcytosis, an endocytic-dependent mechanism involving somatic recycling of TrkA receptors to axons [43, 44]. In this sense, it is possible to hypothesize that Tspan1 could regulate neuronal connectivity by controlling the anterograde trafficking of newly synthesized TrkA receptors to distal axons or by modulating the somatic pool of membrane TrkA that can be recycled to axons by transcytosis. Interestingly, our results open the possibility that tetraspanins may represent key regulators of neurotrophic factor receptor homeostasis, with capacity to regulate their biosynthetic trafficking, degradation, and availability on the cell surface. The proper biosynthetic delivery of TrkA receptors is essential for correct neurotrophin function and disturbances in neurotrophin receptor trafficking have been postulated to contribute to neurodegenerative and neurodevelopmental disorders [45, 46]. In line with this, recent findings also demonstrated that certain TrkA mutations that disrupt autophagy homeostasis causes neurodegeneration [31].

Although the molecular mechanisms through which tetraspanins regulate cellular physiology are not completely known, previous evidence demonstrated that different tetraspanins regulate receptor tyrosine kinase (RTK) activity acting through different mechanisms such as organizers of multi-subunit receptor signaling complexes, receptor trafficking, and ligand-induced receptor dimerization and endocytosis [22].

Future studies focused on how posttranslational modifications such as palmitoylation, N-linked glycosylation, and ubiquitination can promote or attenuate tetraspanin function will contribute to understand the specific mechanisms used by tetraspanins to control receptor signaling. In contrast to other tetraspanins, such as CD9 and CD82, which negatively regulate EGF and Met receptor signaling, [47–49], Tspan1 positively regulates TrkA receptor activity.

The functional characterization of the role of Tspan1 for nervous system development remains to be determined. So far, the only evidence indicates that Tspan1 regulates neural differentiation in the early Xenopus embryo [34]. Therefore, more genetic, biochemical and cellular studies will be necessary to address the physiological contribution of Tspan1 for nervous system development.

Previous studies provided compelling evidence indicating that Tspans control neuronal connectivity functioning as regulators of neurite outgrowth, dendrite development, synapse formation, synaptic transmission, and long-term plasticity [25, 26, 50]. Mutations in Tspans leading to loss-of-function phenotype are relatively rare, probably because many tetraspanins overlap functionally. Nonetheless, specific tetraspanins play critical roles during neuromuscular

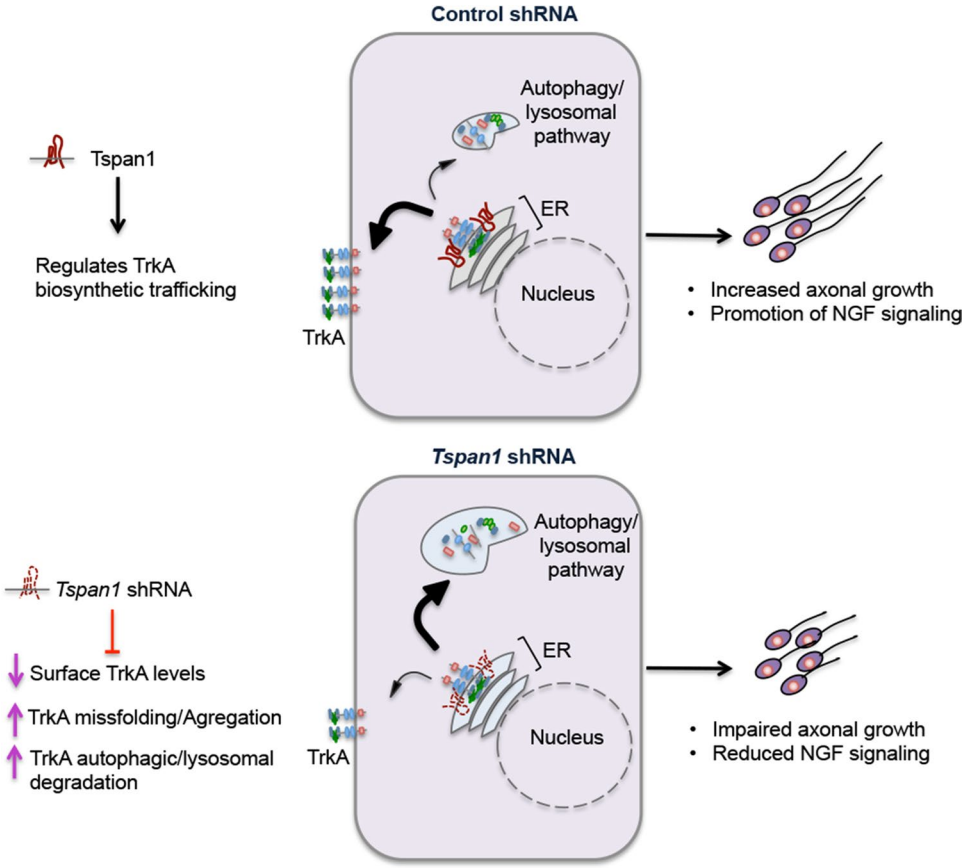

Fig. 9 Model describing the proposed role of Tspan1 in TrkA receptor proteostasis. Tspan1 binds to intracellular TrkA to modulate its biosynthetic trafficking. Functioning as an ER checkpoint quality control, Tspan1 determines the surface expression levels of TrkA, by controlling its sorting to the autophagy/lysosomal degradation pathway. This homeostatic mechanism is crucial in determining neuronal responsiveness to NGF

synapse formation, myelination of peripheral axons, and brain function [16, 51]. Given the crucial role played by tetraspanins in the organization of neuronal connectivity, it seems likely that dysfunctions in these genes or in their binding partners could compromise neuronal function and lead to neurodevelopmental and neurological disorders including intellectual disability and motivation [52]. Mutations in the gene encoding for Tspan6 have been identified in patients with epilepsy-associated with autism [53]. In addition, the deletion of Tspan6 affects basal glutamatergic transmission and long-term potentiation. In hippocampal neurons, Tspan7 regulates AMPAR trafficking and functional maturation of glutamatergic synapses, a neuronal event whose impairment is implicated in intellectual disability [23]. In the dopaminergic system, it was also reported that Tspan7 interacts with the dopamine D2 receptor [24]. In these neurons, Tspan7 deficiency increases the surface expression of the D2 dopaminergic receptor by reducing its internalization, regardless of dopamine treatment. Notably, Tspan17 protects dopaminergic neurons from 6-OHDA-induced neurodegeneration, highlighting its therapeutic potential for treatment of Parkinson disease [54].

Human neurodegenerative diseases are associated with aberrant protein aggregation, and loss of proteostatic mechanisms are likely involved in the pathogenesis of these disorders [55, 56]. Interestingly, a recent study identified Tspan6 as a novel modulator of the amyloid precursor protein (APP) homeostasis, through a mechanism that prevents APP degradation by the lysosomal pathway and leads APP to exosomal secretion [57].

NGF/TrkA signaling is involved in pain transduction mechanisms and plays a key role in many persistent pain states, notably those associated with inflammation [58]. On this basis, our findings raise the possibility that targeting Tspan1 could decrease the cell-surface expression of TrkA, and thereby reduce inflammatory pain. For this reason, it will be important to study further the significance of the interplay between Tspan1 and TrkA activation in vivo. To achieve this, a more detailed analysis of *Tspan1* conditional knockout mice will help to understand the contribution of Tspan1 for inflammatory pain as well as nervous system function and development.

Acknowledgements We thank Dr. Marcal Vilar for TrkA-L213P construct, Dr. Michael G. Tomlinson for different Tspan constructs, Dr David Sabatini for Lamp1-RFP plasmid; Andrea Pecile and Manuel Ponce for animal care, Lic. Nerina Villalba and Dr. Sebastián Giusti for technical assistance, and Innova-T and UBATEC for research grant administration. This work was supported by the Argentine Agency for Promotion of Science and Technology (ANPCyT) PICT2015-3814, PICT2016-1512, PICT2017-4513. GP, FL, and TF were supported by

an Independent Research Career Position from the Argentine Medical Research Council (CONICET). FFR, PAF, and APD were supported by a fellowship from CONICET.

Author contributions Conceived and designed the experiments: FFR, FL, and GP. Performed the experiments and statistical analysis: FFR, PAF, and AD. Analysis and interpretation of the data: FFR, TF, FL, and GP. Wrote the paper: GP.

References

1. Bodmer D, Levine-Wilkinson S, Richmond A, Hirsh S, Kuruvilla R (2009) Wnt5a mediates nerve growth factor-dependent axonal branching and growth in developing sympathetic neurons. J Neurosci 29:7569–7581
2. Gatto G, Dudanova I, Suetterlin P, Davies AM, Drescher U, Bixby JL, Klein R (2013) Protein tyrosine phosphatase receptor type O inhibits trigeminal axon growth and branching by repressing TrkB and Ret signaling. J Neurosci 33:5399–5410
3. Lehigh KM, West KM, Ginty DD (2017) Retrogradely transported TrkA endosomes signal locally within dendrites to maintain sympathetic neuron synapses. Cell Rep 19:86–100
4. Huang EJ, Reichardt LF (2003) Trk receptors: roles in neuronal signal transduction. Annu Rev Biochem 72:609–642
5. Paratcha G, Ledda F (2008) GDNF and GFRalpha: a versatile molecular complex for developing neurons. Trends Neurosci 31:384–391
6. Glebova NO, Ginty DD (2004) Heterogeneous requirement of NGF for sympathetic target innervation in vivo. J Neurosci 24:743–751
7. Lallemend F, Ernfors P (2012) Molecular interactions underlying the specification of sensory neurons. Trends Neurosci 35:373–381
8. Luo W, Wickramasinghe SR, Savitt JM, Griffin JW, Dawson TM, Ginty DD (2007) A hierarchical NGF signaling cascade controls Ret-dependent and Ret-independent events during development of nonpeptidergic DRG neurons. Neuron 54:739–754
9. Patel TD, Jackman A, Rice FL, Kucera J, Snider WD (2000) Development of sensory neurons in the absence of NGF/TrkA signaling in vivo. Neuron 25:345–357
10. Kramer ER, Knott L, Su F, Dessaud E, Krull CE, Helmbacher F, Klein R (2006) Cooperation between GDNF/Ret and ephrinA/EphA4 signals for motor-axon pathway selection in the limb. Neuron 50:35–47
11. Ma L, Tessier-Lavigne M (2007) Dual branch-promoting and branch-repelling actions of Slit/Robo signaling on peripheral and central branches of developing sensory axons. J Neurosci 27:6843–6851
12. Ledda F, Bieraugel O, Fard SS, Vilar M, Paratcha G (2008) Lrig1 is an endogenous inhibitor of Ret receptor tyrosine kinase activation, downstream signaling, and biological responses to GDNF. J Neurosci 28:39–49
13. Mandai K, Guo T, St Hillaire C, Meabon JS, Kanning KC, Bothwell M, Ginty DD (2009) LIG family receptor tyrosine kinase-associated proteins modulate growth factor signals during neural development. Neuron 63:614–627
14. Meabon JS, de Laat R, Ieguchi K, Serbzhinsky D, Hudson MP, Huber BR, Wiley JC, Bothwell M (2016) Intracellular LINGO-1 negatively regulates Trk neurotrophin receptor signaling. Mol Cell Neurosci 70:1–10
15. Franco M, Muratori C, Corso S, Tenaglia E, Bertotti A, Capparuccia L, Trusolino L, Comoglio PM, Tamagnone L (2010) The tetraspanin CD151 is required for Met-dependent signaling and tumor cell growth. J Biol Chem 285:38756–38764
16. Hemler ME (2005) Tetraspanin functions and associated microdomains. Nat Rev Mol Cell Biol 6:801–811
17. Liu Z, Shi H, Szymczak LC, Aydin T, Yun S, Constas K, Schaeffer A, Ranjan S, Kubba S, Alam E et al (2015) Promotion of bone morphogenetic protein signaling by tetraspanins and glycosphingolipids. PLoS Genet 11:e1005221
18. Odintsova E, Sugiura T, Berditchevski F (2000) Attenuation of EGF receptor signaling by a metastasis suppressor, the tetraspanin CD82/KAI-1. Curr Biol 10:1009–1012
19. Odintsova E, Voortman J, Gilbert E, Berditchevski F (2003) Tetraspanin CD82 regulates compartmentalisation and ligand-induced dimerization of EGFR. J Cell Sci 116:4557–4566
20. Tugues S, Honjo S, Konig C, Padhan N, Kroon J, Gualandi L, Li X, Barkefors I, Thijssen VL, Griffioen AW et al (2013) Tetraspanin CD63 promotes vascular endothelial growth factor receptor 2-beta1 integrin complex formation, thereby regulating activation and downstream signaling in endothelial cells in vitro and in vivo. J Biol Chem 288:19060–19071
21. Yanez-Mo M, Barreiro O, Gordon-Alonso M, Sala-Valdes M, Sanchez-Madrid F (2009) Tetraspanin-enriched microdomains: a functional unit in cell plasma membranes. Trends Cell Biol 19:434–446
22. Termini CM, Gillette JM (2017) Tetraspanins function as regulators of cellular signaling. Front Cell Dev Biol 5:34
23. Bassani S, Cingolani LA, Valnegri P, Folci A, Zapata J, Gianfelice A, Sala C, Goda Y, Passafaro M (2012) The X-linked intellectual disability protein TSPAN7 regulates excitatory synapse development and AMPAR trafficking. Neuron 73:1143–1158
24. Lee SA, Suh Y, Lee S, Jeong J, Kim SJ, Kim SJ, Park SK (2017) Functional expression of dopamine D2 receptor is regulated by tetraspanin 7-mediated postendocytic trafficking. FASEB J 31:2301–2313
25. Murru L, Moretto E, Martano G, Passafaro M (2018) Tetraspanins shape the synapse. Mol Cell Neurosci 91:76–81
26. Murru L, Vezzoli E, Longatti A, Ponzoni L, Falqui A, Folci A, Moretto E, Bianchi V, Braida D, Sala M et al (2017) Pharmacological modulation of AMPAR rescues intellectual disability-like phenotype in Tm4sf2-/y mice. Cereb Cortex 27:5369–5384
27. Salas IH, Callaerts-Vegh Z, Arranz AM, Guix FX, D'Hooge R, Esteban JA, De Strooper B, Dotti CG (2017) Correction: Tetraspanin 6: A novel regulator of hippocampal synaptic transmission and long term plasticity. PLoS One 12:e0187179
28. Thiede-Stan NK, Tews B, Albrecht D, Ristic Z, Ewers H, Schwab ME (2015) Tetraspanin-3 is an organizer of the multisubunit Nogo-A signaling complex. J Cell Sci 128:3583–3596
29. Fontanet P, Irala D, Alsina FC, Paratcha G, Ledda F (2013) Pea3 transcription factor family members Etv4 and Etv5 mediate retrograde signaling and axonal growth of DRG sensory neurons in response to NGF. J Neurosci 33:15940–15951
30. Ledda F, Paratcha G, Sandoval-Guzman T, Ibanez CF (2007) GDNF and GFRalpha1 promote formation of neuronal synapses by ligand-induced cell adhesion. Nat Neurosci 10:293–300
31. Franco ML, Melero C, Sarasola E, Acebo P, Luque A, Calatayud-Baselga I, Garcia-Barcina M, Vilar M (2016) Mutations in TrkA causing congenital insensitivity to pain with anhidrosis (CIPA) induce misfolding, aggregation, and mutation-dependent neurodegeneration by dysfunction of the autophagic flux. J Bioll Chem 291:21363–21374
32. Juenger H, Holst MI, Duffe K, Jankowski J, Baader SL (2005) Tetraspanin-5 (Tm4sf9) mRNA expression parallels neuronal maturation in the cerebellum of normal and L7En-2 transgenic mice. J Comp Neurol 483:318–328

33. Tiwari-Woodruff SK, Kaplan R, Kornblum HI, Bronstein JM (2004) Developmental expression of OAP-1/Tspan-3, a member of the tetraspanin superfamily. J Neurosci Res 77:166–173
34. Yamamoto Y, Grubisic K, Oelgeschlager M (2007) Xenopus Tetraspanin-1 regulates gastrulation movements and neural differentiation in the early Xenopus embryo. Differentiation 75:235–245
35. Zemni R, Bienvenu T, Vinet MC, Sefiani A, Carrie A, Billuart P, McDonell N, Couvert P, Francis F, Chafey P et al (2000) A new gene involved in X-linked mental retardation identified by analysis of an X;2 balanced translocation. Nat Genet 24:167–170
36. Watson FL, Porcionatto MA, Bhattacharyya A, Stiles CD, Segal RA (1999) TrkA glycosylation regulates receptor localization and activity. J Neurobiol 39:323–336
37. Berditchevski F, Odintsova E (2007) Tetraspanins as regulators of protein trafficking. Traffic 8:89–96
38. Alsina FC, Ledda F, Paratcha G (2012) New insights into the control of neurotrophic growth factor receptor signaling: implications for nervous system development and repair. J Neurochem 123:652–661
39. Chen B, Zhao L, Li X, Ji YS, Li N, Xu XF, Chen ZY (2014) Syntaxin 8 modulates the post-synthetic trafficking of the TrkA receptor and inflammatory pain transmission. J Biol Chem 289:19556–19569
40. Dornier E, Coumailleau F, Ottavi JF, Moretti J, Boucheix C, Mauduit P, Schweisguth F, Rubinstein E (2012) TspanC8 tetraspanins regulate ADAM10/Kuzbanian trafficking and promote Notch activation in flies and mammals. J Cell Biol 199:481–496
41. Jouannet S, Saint-Pol J, Fernandez L, Nguyen V, Charrin S, Boucheix C, Brou C, Milhiet PE, Rubinstein E (2016) TspanC8 tetraspanins differentially regulate the cleavage of ADAM10 substrates, Notch activation and ADAM10 membrane compartmentalization. Cell Mol Life Sci 73:1895–1915
42. Saint-Pol J, Billard M, Dornier E, Eschenbrenner E, Danglot L, Boucheix C, Charrin S, Rubinstein E (2017) New insights into the tetraspanin Tspan5 using novel monoclonal antibodies. J Biol Chem 292:9551–9566
43. Scott-Solomon E, Kuruvilla R (2018) Mechanisms of neurotrophin trafficking via Trk receptors. Mol Cell Neurosci 91:25–33
44. Yamashita N, Joshi R, Zhang S, Zhang ZY, Kuruvilla R (2017) Phospho-regulation of soma-to-axon transcytosis of neurotrophin receptors. Dev Cell 42(626–639):e625
45. Bronfman FC, Escudero CA, Weis J, Kruttgen A (2007) Endosomal transport of neurotrophins: roles in signaling and neurodegenerative diseases. Dev Neurobiol 67:1183–1203
46. Salehi A, Delcroix JD, Mobley WC (2003) Traffic at the intersection of neurotrophic factor signaling and neurodegeneration. Trends Neurosci 26:73–80
47. Mela A, Goldman JE (2013) CD82 blocks cMet activation and overcomes hepatocyte growth factor effects on oligodendrocyte precursor differentiation. J Neurosci 33:7952–7960
48. Murayama Y, Shinomura Y, Oritani K, Miyagawa J, Yoshida H, Nishida M, Katsube F, Shiraga M, Miyazaki T, Nakamoto T et al (2008) The tetraspanin CD9 modulates epidermal growth factor receptor signaling in cancer cells. J Cell Physiol 216:135–143
49. Tang M, Yin G, Wang F, Liu H, Zhou S, Ni J, Chen C, Zhou Y, Zhao Y (2015) Downregulation of CD9 promotes pancreatic cancer growth and metastasis through upregulation of epidermal growth factor on the cell surface. Oncol Rep 34:350–358
50. Davenport EC, Pendolino V, Kontou G, McGee TP, Sheehan DF, Lopez-Domenech G, Farrant M, Kittler JT (2017) An essential role for the tetraspanin LHFPL4 in the cell-type-specific targeting and clustering of synaptic GABAA receptors. Cell Rep 21:70–83
51. Ishibashi T, Ding L, Ikenaka K, Inoue Y, Miyado K, Mekada E, Baba H (2004) Tetraspanin protein CD9 is a novel paranodal component regulating paranodal junctional formation. J Neurosci 24:96–102
52. Humeau Y, Gambino F, Chelly J, Vitale N (2009) X-linked mental retardation: focus on synaptic function and plasticity. J Neurochem 109:1–14
53. Vincent AK, Noor A, Janson A, Minassian BA, Ayub M, Vincent JB, Morel CF (2012) Identification of genomic deletions spanning the PCDH19 gene in two unrelated girls with intellectual disability and seizures. Clin Genet 82:540–545
54. Masoudi N, Ibanez-Cruceyra P, Offenburger SL, Holmes A, Gartner A (2014) Tetraspanin (TSP-17) protects dopaminergic neurons against 6-OHDA-induced neurodegeneration in *C. elegans*. PLoS Genet 10:e1004767
55. Cheng J, North BJ, Zhang T, Dai X, Tao K, Guo J, Wei W (2018) The emerging roles of protein homeostasis-governing pathways in Alzheimer's disease. Aging Cell 17(5):e12801. https://doi.org/10.1111/acel.12801
56. Hartl FU, Bracher A, Hayer-Hartl M (2011) Molecular chaperones in protein folding and proteostasis. Nature 475:324–332
57. Guix FX, Sannerud R, Berditchevski F, Arranz AM, Horre K, Snellinx A, Thathiah A, Saido T, Saito T, Rajesh S et al (2017) Tetraspanin 6: a pivotal protein of the multiple vesicular body determining exosome release and lysosomal degradation of amyloid precursor protein fragments. Mol Neurodegener 12:25
58. Yu T, Calvo L, Anta B, Lopez-Benito S, Lopez-Bellido R, Vicente-Garcia C, Tessarollo L, Rodriguez RE, Arevalo JC (2014) In vivo regulation of NGF-mediated functions by Nedd4-2 ubiquitination of TrkA. J Neurosci 34:6098–6106